

LED backlight designs with the flow-line method

Dejan Grabovičkić,^{1,*} Pablo Benítez,^{1,2} Juan C. Miñano,^{1,2} and Julio Chaves²

¹*Escuela Técnica Superior de Ingenieros de Telecomunicación, Universidad Politécnica de Madrid (UPM), Avenida Complutense 30 28040 Madrid, Spain*

²*LPI 2400 Lincoln Ave., Altadena, California 91001, USA*

**dejan@cedint.upm.es*

Abstract: An LED backlight has been designed using the flow-line design method. This method allows a very efficient control of the light extraction. The light is confined inside the guide by total internal reflection, being extracted only by specially calculated surfaces: the ejectors. Backlight designs presented here have a total optical efficiency of up to 80% (including Fresnel and absorption losses) with an FWHM below 30 degrees. The experimental results of the first prototype are shown.

©2011 Optical Society of America

OCIS codes: (080.4298) Nonimaging optics; (220.2945) Illumination design.

References and links

1. J. C. Miñano, P. Benítez, J. Chaves, M. Hernández, O. Dross, and A. Santamaría, "High-efficiency LED backlight optics designed with the flow-line method," *Proc. SPIE* **5942**, 594202, 594202-12 (2005).
 2. D. Feng, G. Jin, Y. Yan, and S. Fan, "High quality light guide plates that can control the illumination angle based on microprism structures," *Appl. Phys. Lett.* **85**(24), 6016–6018 (2004).
 3. D. Feng, Y. Yan, X. Yang, G. Jin, and S. Fan, "Novel integrated light-guide plate for liquid crystal display backlight," *J. Opt. A, Pure Appl. Opt.* **7**(3), 111–117 (2005).
 4. H. Tanase, J. Mamiya, and M. Suzuki, "A new backlighting system using a polarizing light pipe," *IBM J. Res. Develop.* **42**(3), 527–536 (1998).
 5. N. Guselnikov, P. Lazarev, M. Paukshto, and P. Yeh, "Translucent LCDs," *J. Soc. Inf. Disp.* **13**(4), 339–348 (2005).
 6. S. R. Park, O. J. Kwon, D. Shin, S. H. Song, H. S. Lee, and H. Y. Choi, "Grating micro-dot patterned light guide plates for LED backlights," *Opt. Express* **15**(6), 2888–2899 (2007).
 7. W. J. Cassarly, "Backlight pattern optimization," *Proc. SPIE* **6834**, 683407, 683407-12 (2007).
 8. K. Imai and I. Fujieda, "Illumination uniformity of an edge-lit backlight with emission angle control," *Opt. Express* **16**(16), 11969–11974 (2008).
 9. R. Winston, J. C. Miñano, and P. Benítez, with contributions of N. Shatz and J. Bortz, *Nonimaging Optics* (Elsevier, Academic Press, 2004).
-

1. Introduction

Most existing LCDs are still backlit with a cold cathode fluorescent lamp (CCFL). These lamps are efficient in terms of light output, but LEDs are progressively gaining market share. LEDs have many advantages over the fluorescent lamps which is propelling this progression: the possibility of dynamic electronic control of the illumination for a lower power consumption and higher contrast, higher compactness, less weight, less voltage, greater reliability, instant start up, larger colour range and brightness. These advantages have made them ideal for many applications including monitors in notebook personal computers, screens for TV, and many portable information terminals.

To satisfy market trends, it is important to make backlights as an efficient, thin, light, and bright system. There are many backlight designs that fulfill these requirements [1–8], which are designed using optimization algorithms and non-deterministic management of the light (via random scatterers), which usually sacrifice efficiency. In this paper we present several designs using the flow-line design method of Nonimaging Optics introduced in [1], which provides a deterministic efficient control of the light, together with the experimental results of the first manufactured prototype

2. Backlight architecture

Figure 1 shows the cross section of our LED backlight architecture. It consists of two sections: a collimator and a beam slicer. In fact, both functions can be integrated into just one section [1], but are considered separately for simplicity. In the 2D cross section, the top line of the beam slicer is labeled as “top guide line”, since it guides the light all along the backlight, while the bottom line of the beam slicer is a microstructured line made up of two alternating segments, labeled as “guide segments” and “ejectors” (Fig. 1). The ejectors “slice” the incoming bundle into small “light ribbons”, which are ejected with high collimation ($\sim 20^\circ$ - 30° FWHM) through the top guide line toward the LCD. The input rays need to be collimated enough so that all of them are totally internally reflected when they hit the top guide line, guide segments or ejectors. This is done by a collimator at the entrance of the slicer (for example a CPC).

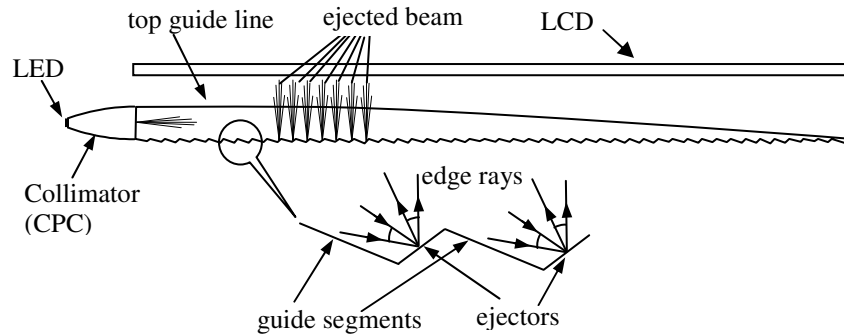


Fig. 1. Cross section of a generalized LED backlight design based on the flow-line method.

3. Extended ray bundles and flow lines

Let the refractive index of the backlight, n , be known, and let the collimator illuminates the beam slicer (in the cross section of Fig. 1) within an angle $\pm \theta$. For the beam slicer design, consider an extended bundle of rays passing through the segment AB within an angle $\pm \theta$ with respect to the x axis. The edge rays of that extended bundle [9] are shown in Fig. 2. For clarity, they have been represented as two subsets. Every point in the region bounded by the rays r_1 and r_2 is crossed by two edge rays (one ray of each edge ray subset). These subsets can be defined by two eikonal functions $O_1(x,y)$ and $O_2(x,y)$, whose constant values provide the wavefronts associated to those edge ray subsets.

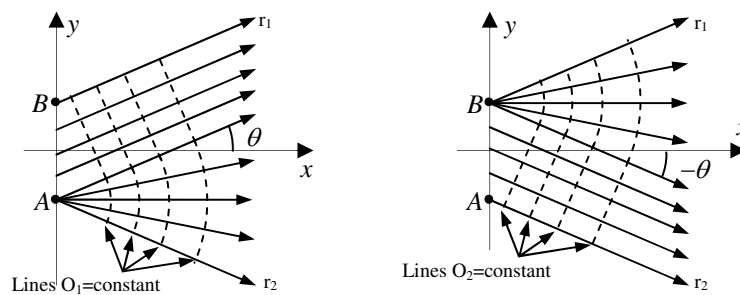


Fig. 2. Edge rays of the bundle immersed in a medium of refractive index n and radiating from the strip AB within the angle $\pm \theta$.

The $j = \text{const}$ lines of the function

$$j(x, y) = \frac{O_1(x, y) - O_2(x, y)}{2} \quad (1)$$

are the well-known flow lines of the bundle [1,9]. At each point they bisect the angle formed between the two edge rays at that point. Figure 3(a) shows the flow lines for the edge rays presented in Fig. 2. The flow lines have two useful properties [9]. First, since they bisect the bundle, a reflector can be placed coincident with the flow line without modifying the extended ray bundle as a whole: the edge rays associated to eikonal O_2 are just transformed into edge rays associated to eikonal O_1 . This property will be used to design the top guide line and the guide segments of the bottom microstructured line to coincide with the flow lines.

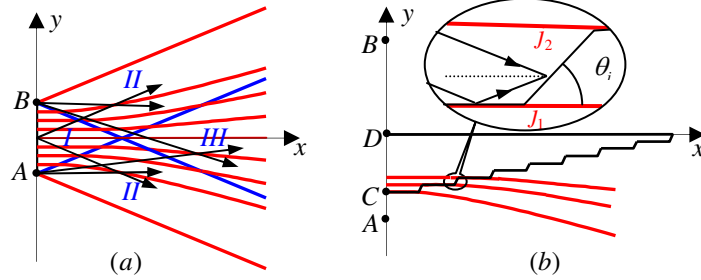


Fig. 3. Flow lines for the beam radiating from the strip AB (in red), (a) Definition of the flow lines, (b) Design procedure for the conical and linear backlights.

The second interesting property of the flow lines is that the étendue ΔE of the rays crossing a segment whose edge points lay on flow lines j_1 and $j_2 > j_1$ is independent of the coordinates of those points (see Fig. 3(b)), and is just given by:

$$\Delta E = 2(j_2 - j_1) \quad (2)$$

The ejectors can be designed to reflect the rays, so the flow lines after the reflection are essentially perpendicular to the x -axis. Then the rays will be refracted at the top guide line, but since this line will be selected parallel or nearly parallel to the x -axis, the flow lines of the refracted bundle will remain essentially perpendicular to the x -axis.

Therefore, if all the rays have the same radiance R , the incremental power is $\Delta P = R\Delta E = 2R\Delta j$. In order to provide uniform irradiance on the LCD ($dP/dx = \text{constant}$), the envelope of the microstructured line (at the limit of infinitesimally small ejectors), must fulfill the equation:

$$\frac{dj(x, y)}{dx} = \text{constant} = \frac{E_{out}}{2l} \quad (3)$$

where E_{out} is the 2D étendue of the exiting bundle. Extrapolated to finite ejector sizes, Eq. (3) means that, for instance, if all the ejectors have the same projected size Δx , each ejector must intercept the same Δj .

By introducing the equation of the envelope of the microstructured line as $y = y(x)$ in Eq. (3), it will fulfill the following differential equation:

$$\frac{\partial j}{\partial x} + \frac{\partial j}{\partial y} y' = \frac{E_{out}}{2l} \quad (4)$$

4. Beam slicer design in two-dimensions

The design procedure consists of four steps: (1) choice of the ray bundle, (2) calculation of its flow lines, (3) selection of one flow line as the top guide line and (4) construction of the

microstructured line. In this paper, we will present two designs (called *conical* and *linear*), both associated with the ray bundles already presented in Fig. 3(a), so step (1) is completed. For step (2), the flow lines in Fig. 3(a) consist of 3 segments (with C^1 continuity): a straight line (in region I of Fig. 3(a)), a parabola (in region II), and a hyperbola (in region III). This can be easily obtained by calculating the lines bisecting the edge rays in each region. In region I each point is intercepted by two edge rays forming the angle θ in respect to the axis x , thus the flow lines are straight lines $y = \text{const}$. In region II, one edge ray comes from an interior point of the strip AB , while the other from an extreme point of the strip (A or B). Therefore, the flow lines are the parabolas with focus at A or B . Finally, in region III both edge rays come from points A and B , so the flow lines become the hyperbolas with foci A and B .

In step (3), for both designs, we will select the flow line $y = 0$ as the top guide line. Finally, in step (4) the microstructured line must be calculated. For very small ejector sizes, this could be done by solving differential Eq. (4) with contour condition $y(0) = -d_0$, where d_0 is the collimator exit aperture size (in Fig. 3 the aperture is given by the strip CD). However, for better performance, we do the exact finite-facet construction. This is implemented by starting from the flow line passing through point $C = (0, -d_0)$, alternating flow line segments (which are the guide lines) and the ejectors. We chose that these ejectors will all intercept the same étendue Δ_j , and with a tilt provided that all the rays are reflected by total internal reflection.

The input parameters for the finite facet-size design are the coordinate y_0 that defines points $A = (0, y_0)$ and $B = (0, -y_0)$, the aperture size d_0 and angle θ of the collimation, the minimum thicknesses of the beam slicer at its end, d_{\min} , which is fixed by manufacturing constraints. The purely geometrical efficiency (i.e., without considering absorption or Fresnel losses) is given by the ratio $E_{\text{out}}/E_{\text{in}}$, where $E_{\text{in}} = 2 \cdot n \cdot d_0 \cdot \sin \theta$ is the étendue of the bundle exiting the collimator and entering the beam slicer. Note that fixing $d_{\min} > 0$ implies some geometrical losses, given by E_l , escaping at the end of the slicer ($E_l = E_{\text{in}} - E_{\text{out}}$).

Once the design is finished, the maximum thickness of the beam slicer, d_{\max} , and the length l are computed. Since d_{\max} and l are more practical input parameters, we match them by varying d_0 and θ .

When y_0 is small enough that flow lines inside the beam slicer contain not only straight line segments but parabolic and hyperbolic ones too (i.e. the slicer is designed in regions I-III), the design will be called *conical backlight* here. When y_0 tends to infinity, the bundle has only region I, so all the flow lines inside the beam slicer are straight lines, therefore the design will be called *linear backlight*.

Figure 4 shows the cross section of two of these designs. The conical one has been designed with the following specifications: $AB = 5\text{mm}$, $\theta = 10^\circ$, $d_{\min} = 0.5\text{mm}$, $d_{\max} = 2.9\text{mm}$, $p = 1\text{mm}$ (where d_{\min} and d_{\max} are the smallest and the biggest thicknesses, and p is the distance between two ejectors). A linear backlight design with similar specifications: $\theta = 8^\circ$, $d_{\min} = 0.5\text{mm}$, $d_{\max} = 2.89\text{mm}$, $p = 1\text{mm}$ is also modeled.



Fig. 4. Cross section of designed models, (a) conical backlight, (b) linear backlight.

5. Three-dimensional designs

Figure 5 shows the 3D model of the one of the backlights obtained by linear symmetry along the z -axis of both the beam slicer and collimator sections. We have selected this simple symmetry to ease the prototype manufacturing (see Section 6). The LEDs will not be glued to the collimators, which will have a flat entry surface. Therefore, the light after the refraction will form an angle with the x -axis smaller than the critical angle. Note that due to the linear

symmetry of the collimators, the light exiting the backlight towards the LCD plane will be collimated only in the x - y plane, but not in the z - y . Collimation in both directions can be obtained using cross-CPC type collimators (which collimate in both dimensions) and the same linear-symmetric beam slicer.

The conical design has been traced in a commercial raytrace package LightTools®, using 7 equally spaced LEDs with dimensions $0.6 \times 1.9 \text{ mm}$ (the same dimensions as OSRAM microside LEDs). Beside the collimation, the collimator's function is to mix the rays coming from different LEDs, so that the irradiance at the entrance of the slicer is uniform. This provides an equal etendue supply for the ejectors.

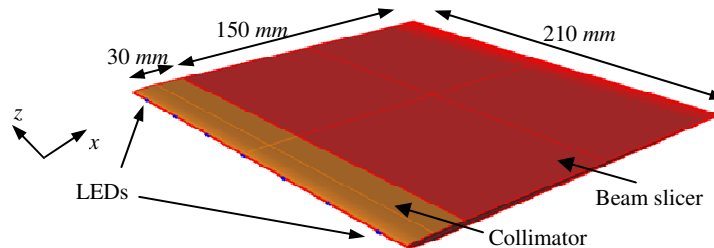


Fig. 5. 3D view of the LED backlight optics.

The LightTools® simulation gives 92.0% of geometric efficiency and 79.9% of total efficiency (including Fresnel and absorption losses) for the conical backlight, and 82.0% of geometric efficiency and 71.4% of total efficiency for the linear backlight.

6. Simulations and experimental results for a linear backlight prototype

Considering the efficiency, the best design presented here is the conical backlight. However, the linear backlight is easier and cheaper to prototype since its microstructure lines consist of straight lines, the thickness decreases constantly and all the ejectors have the same size (in this design, 22 microns of horizontally projected dimension). Therefore, we have chosen the linear backlight design for the first prototype (Fig. 6), manufacturing direct cutting of the PMMA, and using 7 OSRAM microside LEDs.

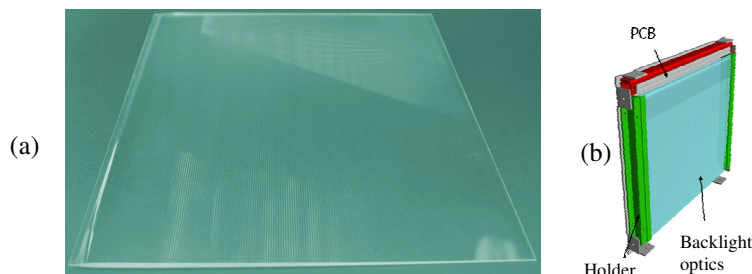


Fig. 6. (a) Manufactured linear backlight. (b) 3D model of the manufactured prototype assembly.

The edge of the prototype has been observed under a microscope. It has been noticed that the curvature radii at the connection between guiding lines and ejectors is around $10 \mu\text{m}$, which must certainly affect the performance. Therefore, an approximate model with all of the edges having the same radius of curvature of $10 \mu\text{m}$ has also been simulated. The surface scattering is considered as negligible. The simulation shows an irradiance pattern with the maximum variation (in respect to the mean value) of 10.7% (Fig. 7(a)), and an efficiency of 61.2%. These values are poorer than the 6.8% non-uniformity and 71.4% efficiency predicted with the idealized model (with null radius) mentioned in Section 4. The simulated intensity

distribution of the realistic model is also shown in Fig. 7(b), in which the lack of collimation in one dimension can be appreciated due to the selected linear symmetry of the collimators.

The experimental measurements of the irradiance at the backlight exit have been carried out with a luxmeter placed at seventeen points distributed throughout the prototype's exit aperture. These measurements show a non-uniformity of about 12%, compared to the 10.7% predicted by the simulation. This disagreement may be due to dispersion of flux between the 7 LED's.

The prototype's intensity distribution and optical efficiency were measured using a single LED and the LUCA optics measurement system. This system comprises a camera, lens, screen and software that processes the information collected by the CCD camera (Fig. 8). Since the camera aperture is very small, we can consider that the screen is placed at infinity from the camera, so the CCD directly reflects the power emitted by each point on the screen. The screen is located on the lens's focal plane thus the parallel rays from the source will focus on a point on the screen. The camera records the power of the light at each point on the screen. From this data the overall power has been calculated.

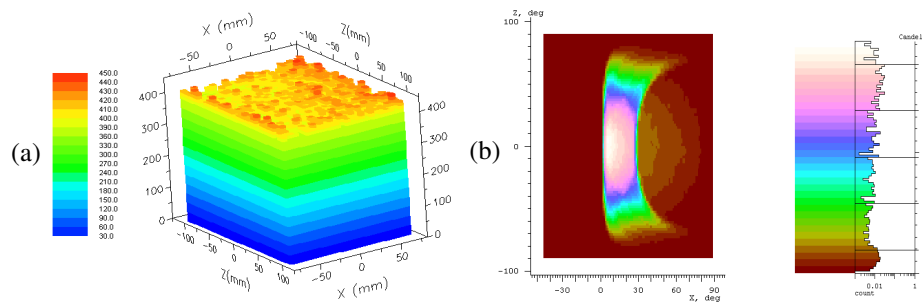


Fig. 7. (a) Simulated irradiance distribution. (b) Intensity distribution of the prototype.

Due to the sizes of backlight and Luca's lens, one measurement can involve only the light contained in a range of $\pm 5^\circ$ and $\pm 10^\circ$. In order to measure the total output radiation, the backlight was set on the platform of a two-axis rotator and rotated from -90° to 90° in both axes with steps of 10° and 20° , as shown in Fig. 8. The measured efficiency is 51.7%. The additional efficiency drop of 10% (in respect to the simulated value 61.2%) is caused by surface roughness and coupling losses between the LEDs and the backlight.

The measured and simulated cross section of the intensity distribution is also shown on the right-hand side of Fig. 8(b), which shows a reasonable agreement, and a FWHM $< 30^\circ$. The intensity has been designed with an offset of 15° with respect to the normal to the backlight to guarantee the total internal reflections of the ejectors.

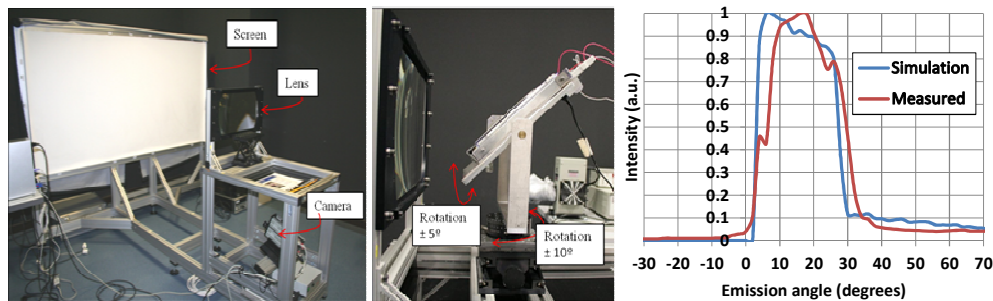


Fig. 8. LUCA measurement system, and simulated and measured intensity cross section profiles.

7. Summary

The presented backlight designs contain a basic piece called a beam slicer which guides the beam between flow lines and periodically ejects a part of it, creating an output beam which is made up of small ribbons of light. All of the designs provide uniform radiation for the LCD with high efficiency (up to 80% including all losses). The experimental results differ from the theoretical results due to surface errors and roughness.

Acknowledgments

The authors thank the Spanish Ministries MCINN (DEFFIO: TEC2008-03773), MITYC (ECOLUX: TSI-020100-2010-1131, SEM: TSI-020302-2010-65), the Madrid Regional Government (SPIR: 50/2010O.23/12/09, TIC2010 and O-PRO: PIE/209/2010) and UPM (Q090935C59) for the support given in the preparation of the paper. The authors also thank Synopsys for granting us the LightTools[®] university license.